Alloxazine-Based Ligands Appended with Coordinating Groups: Synthesis, Electrochemical Studies, and Formation of Coordination Polymers

Jaison Casas, David Pianca, Nolwenn Le Breton, Abdelaziz Jouaiti, Christophe Gourlaouen, Marine Desage-El Murr, Steven Le Vot, Sylvie Choua, Sylvie Ferlay

Alloxazine based ligands appended with coordinating groups: synthesis, electrochemical studies and formation of Coordination Polymers

Jaison Casas,[a] David Pianca,[b] Nolwenn Le Breton,[b] Abdelaziz Jouaiti,[a] Christophe Gourlaouen,[b] Marine Desage-El Murr,[b] Steven Le Vot,[c,d] Sylvie Choua,[b] Sylvie Ferlay[a]*

a CNRS, CMC UMR 7140, Université de Strasbourg, 4 rue Blaise Pascal, CS 90032, Strasbourg, 67081 Cedex, France

b Institut de Chimie, UMR CNRS 7177, Université de Strasbourg, Institut Le Bel, 4 rue Blaise Pascal, Strasbourg, 67000, France

c Institut Charles Gerhardt Montpellier (ICGM), Univ. Montpellier, CNRS, ENSCM, Montpellier, 34000, France

d Réseau sur le Stockage Électrochimique de l'Énergie (RS2E), CNRS, Amiens, 80000, France

* Email: ferlay@unistra.fr

ABSTRACT.

Three new ligands based on the alloxazine core appended with pyridyl coordinating groups have been designed, synthesized and characterized. The ligands reveal to be redox-active in DMF solution, as attested by CV and combined CV/EPR studies. The spin of the reduced species appears to be delocalized on the alloxazine core, as attested by DFT calculations. The coordination abilities of one of the ligands towards Cu^{2+} or Ni^{2+} 3d cations revealed the formation of the first alloxazine-based 3D coordination polymers, presenting strong pi-pi stacking and substantial cavities. Preliminarily charge/discharge experiments in Li-Batteries evidence the Li^{+} insertion in such systems.

Redox-active Porous Coordination Polymers (PCPs) and Metal Organic Frameworks MOFs are the subject of development in the recent years,[1,2] both at the fundamental and experimental level. Redox-active CPs and MOFs[3,4,5] present the ability to allow electron transfers in three directions of space, which gives them interesting properties and possible applications in the field of electrocatalysis,[6,7] or as photo- and electrochromic materials and devices made from conductive MOFs[8,9,10,11] for example.

For the formation of Redox-active PCPs, many strategies have been successfully developed, for example using the combination of Redox active ligands with metals and/or Redox active guests in the formed porous network. Different families of organic ligands have been intensively used for the formation of new redox-active PCPs : ligands derivatives from viologens,[12] guanidines,[13] tetrathiafulvalene (TTF),[14,15] thiazolo[5,4-d]thiazole (TzTz)[16] or naphthalene diimides (NDIs).[17] The formed extended molecular compounds present properties such as photochromism, they can also present charge transfer or be electroactive materials.

Alloxazines, isomers of isoalloxazine related to flavins[18] belong to an important class of biomolecules exhibiting three different redox and protonation states including an intermediate radical state.[19] They have been known to perform chelation of various metal ions through 4-O and 5-N site of the alloxazine core.[20] Complexes of alloxazine coordinated through the O,N alloxazine core with transition metals have been reported mostly with 4d and 5d metals such as ruthenium, rhenium, iridium and tungsten. The first coordination polymers based on the parent isoalloxazine with Ag^{+} cations and not with 3d metals, have been recently reported, and involve the coordination to O,N atoms of the flavin core, and the formation of a five-membered α-iminoketo chelate ring-like.[21,22]

The flavins (isoalloxazine) and their isomers have attracted much attention in the recent years in the fields of catalysis and also energy storage.[23,24] Several chemical modifications have been performed to this core: among them, a pioneering work reported the development of a catechol-alloxazine hybrid redox-active ligand with interesting coordination modes[25] and redox-active catalytic properties to these molecules and complexes.[26] Further chemical development for bringing new coordination abilities to the alloxazine core have not been reported so far in the literature and are reported here..

Here below, we introduce a new class of coordinating of alloxazine based-ligands, where the alloxazine core has been decorated with pyridine coordinating groups (figure 1). The electrochemical properties of these species have been investigated in solution, and their coordination abilities have been studied, evidencing the formation of new Coordination Polymers (CPs), together with preliminarily charge/discharge behavior in Li-batteries.

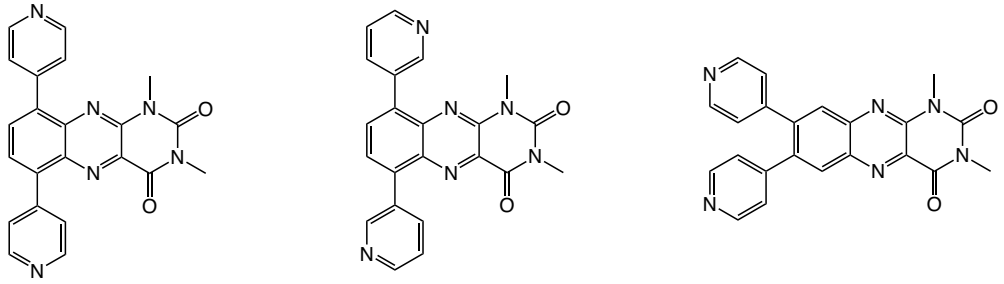

L1 **L2** **L3**

Figure 1: Molecular design for alloxazine based ligands **L1**-**L3**

The design of new candidates is based on the use of the 6,9 and 7,8 carbon positions of the alloxazine core. Ligands **L1**-**L3** (Figure 1) have been obtained in three steps (see Scheme S1 in SI) by condensation of alloxane with 3,6-dibromobenzo-1,2-diamine (**1**) or 4,5-dibromobenzo-1,2-diamine (**1'**) in the presence of boric acid, to provide dibromo

intermediates **2** or **2'** respectively, that were methylated using methyl iodide, leading to **3** or **3'** respectively (scheme S1 in SI). Then a Suzuki-Miyaura cross-coupling was carried out with 4-pyridyl in order to obtain **L1** and **L3**, or 3-pyridyl in order to obtain **L2**. **L1-L3**, were characterized in solution using NMR and MS spectroscopies (see experimental part in SI). Crystals of **L3** have been obtained upon slow evaporation and its structure has been solved. Attempts to obtain suitable single crystals for XRD resolution for ligands **L1** and **L2** failed.

The crystal structure of **L3** revealed the presence of the neutral ligand **L3** without any solvents in the unit cell. The compound (Figure S1 a in SI) crystallizes in the monoclinic $C2/c$ space group (see crystallographic Table S1 in SI) and presents the formula: $C_{22}H_{16}N_6O_2$. The C-N distances of the central pyrazine adjacent to the alloxazine moiety are attesting the alloxazine character of the molecule[27] and not isoalloxazine (see Table S2 in SI). The pyridyl rings are tilted with an angle of 56.071° and 35.24°compared to the plane formed by the flat alloxazine core. As shown in Figure S1b in SI, strong π–π stacking between the phenyl rings of the alloxazine moieties is observed with a 3.475 Å distance between the pyridyl and alloxazine cores.

L1-**L3** are poorly soluble in many organic solvents but highly soluble in DMF, which was chosen for the electrochemical studies. Their redox properties were studied by electrochemical methods in DMF solutions.

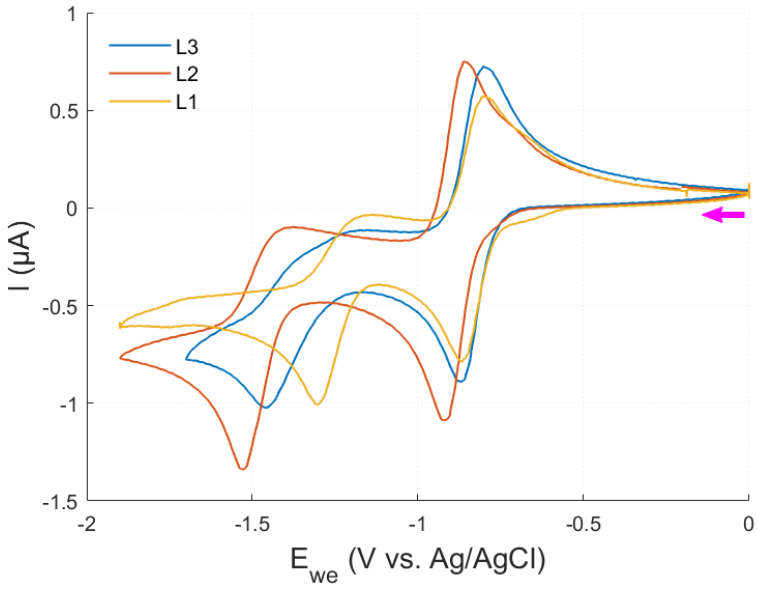

Figure 2: Cyclic voltammograms of 1 mM **L1**, **L2** and **L3** recorded in DMF with 0.1 M $TBABF_4$: working electrode = glassy carbon, Reference Electrode= $Ag/AgCl_{sat}$, counter electrode = Pt. Scan rate: 40 mV s-1.

Cyclic voltammetry (CV) on a glassy carbon electrode in DMF solutions with tetrabutylammonium tetrafluoroborate ($TBABF_4$ 0.1 M) as supporting electrolyte was performed for **L1**-**L3**. The first reduction wave appears at E_{Red1}= −0,80 V for **L1**, E_{Red1}= −0.86 V for **L2** and at E_{Red1} = −0.81 for **L3** (RE: $Ag/AgCl_{sat}$), as shown in Figure 2 and could be attributed to the formation of the radical species. The second less reversible reduction wave following the first one can be attributed to the formation of the doubly reduced species, as already observed for flavin mononucleotide.[25,28,29] For the three ligands, the significantly more negative potential required to perform the second reduction, combined to the irreversibility of the associated redox wave, strongly suggests that the doubly reduced compounds is an unstable specie.

Electrochemical reduction coupled to EPR spectroscopy was then used to generate the intermediate radical anions with the appropriate redox potential previously determined by CV. Well-resolved X-band EPR spectra consisting of eight lines were recorded at room temperature (see Figure 3a-c for **L1**-**L3**). They were attributed to the radical anions with *g* values close to the ones of the free electron (g_e = 2.0023) and thus indicative of the presence of an organic radical. Note that these species are stable over several hours. Simulations of spectra revealed hyperfine coupling (hfccs) with to two sets of one nitrogen (^{14}N) and one set of one proton (^{1}H) (see Table 1 for EPR parameters). To assign the proton and nitrogen atoms, hfccs DFT calculations were carried out (see experimental section in SI for details). Geometry optimizations and calculations of the isotropic Fermi contact coupling were achieved and allowed for the assignment of hfccs determined experimentally.

The DFT optimized geometries and the Singly Occupied Molecular Orbital (SOMO) are shown in Figure 3d-f for **L1**-**L3**. The unpaired electron is mainly delocalized over the phenazine nitrogen atoms and occupies an antibonding orbital. The SOMO is also partially extended on the neighboring C-H group leading to high amplification of A_H value in the EPR spectra, as shown by the values provided in Table 1.

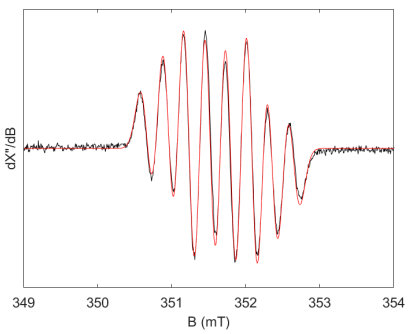

a L1

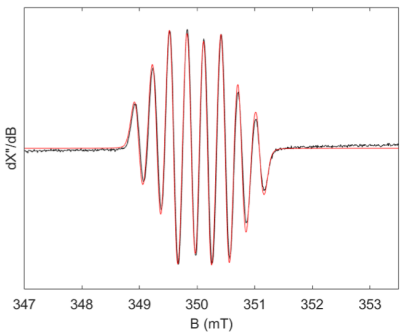

b L2

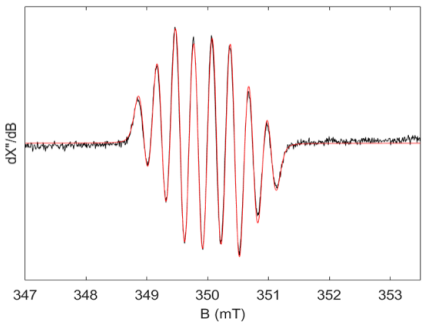

c L3

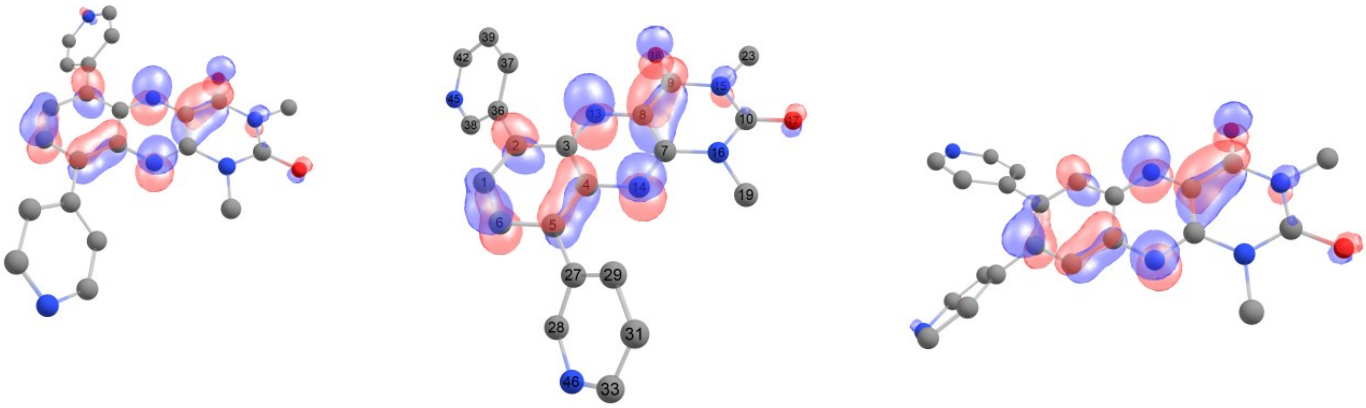

d L1 **e L2** **f L3**

Figure 3: For **L1**-**L3**: a-c) X-Band EPR spectrum of 1 mM electrochemically generated one-electron reduced species, Solid black line: experimental, red line: simulation using parameters in Table 1 (Power = 5 or 6mW; Microwave frequency = 9.81 or 9.86 GHz; modulation frequency=100 kHz, modulation 1G, number of scans=15 and d-f) SOMO calculated by DFT for the one-electron reduced ligand, and numbering of the atoms of the alloxazine core (fore **L2**).

Compound	A (^{14}N) exp/cal	A (^{14}N) exp/cal	A (^{1}H6 or ^{1}H8) exp/cal
L1	15.7/19.0	7.8/9.5	8.4/10.0
L2	16.5/20.0	8.2/9.7	9.2/10.0
L3	16.8/20.3	8.6/10.2	8.0/10.0

Table 1: DFT-calculated hyperfine coupling constants (hfccs, MHz) and comparison with experimental value in MHz (EPR data).

The coordination abilities of **L1** were then tested and when **L1** is combined with a metallic salt $M^{II}(NO_3)_2.x\,H_2O$ (M = Cu or Ni) in ambient conditions (slow diffusion technique),

single crystals of M**L1**$(NO_3)_2$ (M = Cu or Ni) were obtained, see experimental part in SI. Other attempts to obtain diffracting single crystals using **L2** and **L3** failed.

The structure refinement was obtained for Ni**L1**$(NO_3)_{2,}$ while the crystals of Cu**L1**$(NO_3)_2$ were poorly diffracting and only the cell parameters could be refined, attesting the isomorphous character between Ni**L1**$(NO_3)_{2,}$ and Cu**L1**$(NO_3)_2$, presenting the same metrics (see Table S1 in SI), which is isostructurality. The XRD analysis revealed the formation of two isostructural compounds crystallizing in the monoclinic $C2/c$ space group (see crystallographic Table S1 in SI) and presenting the formula $(C_{22}H_{16}N_6O_2)M^{II}(NO_3)_2$ (M = Cu or Ni) and the general formula is **L1**$M^{II}(NO_3)_2$.mS (M = Cu or Ni and S = solvents) (named here M**L1**$(NO_3)_2$); the quality of the crystals did not allow to refine the solvent molecules and the disordered nitrate moieties, so that the squeeze command[30] was applied. Both compounds behave as 2D compound bridged by NO_3^- moieties, leading to porous 3D compounds. In Ni**L1**$(NO_3)_2$, four **L1** moieties are coordinating Ni^{2+} ions in the basal plane through N atoms from the pyridyl moiety, forming thus a 2D grid as shown in Figures 4 and S2 b in SI and the grids are interconnected by disordered NO_3^- anions acting as bridges between the grids (as shown in Figure S2 a in SI), so that the environment of the octahedral Ni^{2+} cations is N_4O_2 (see Table S3 in SI for bond and distances). The grids are not superposing, which allows a π–π stacking between the phenyl rings of the alloxazine moieties with distances of 3.462 Å, as displayed by the "double grids" shown in Figure 4.

Ni**L1**$(NO_3)_2$ is thus PCP, and the diameter of the cavities can be estimated to 10.8Å (see yellow spheres in **Figure 4**).

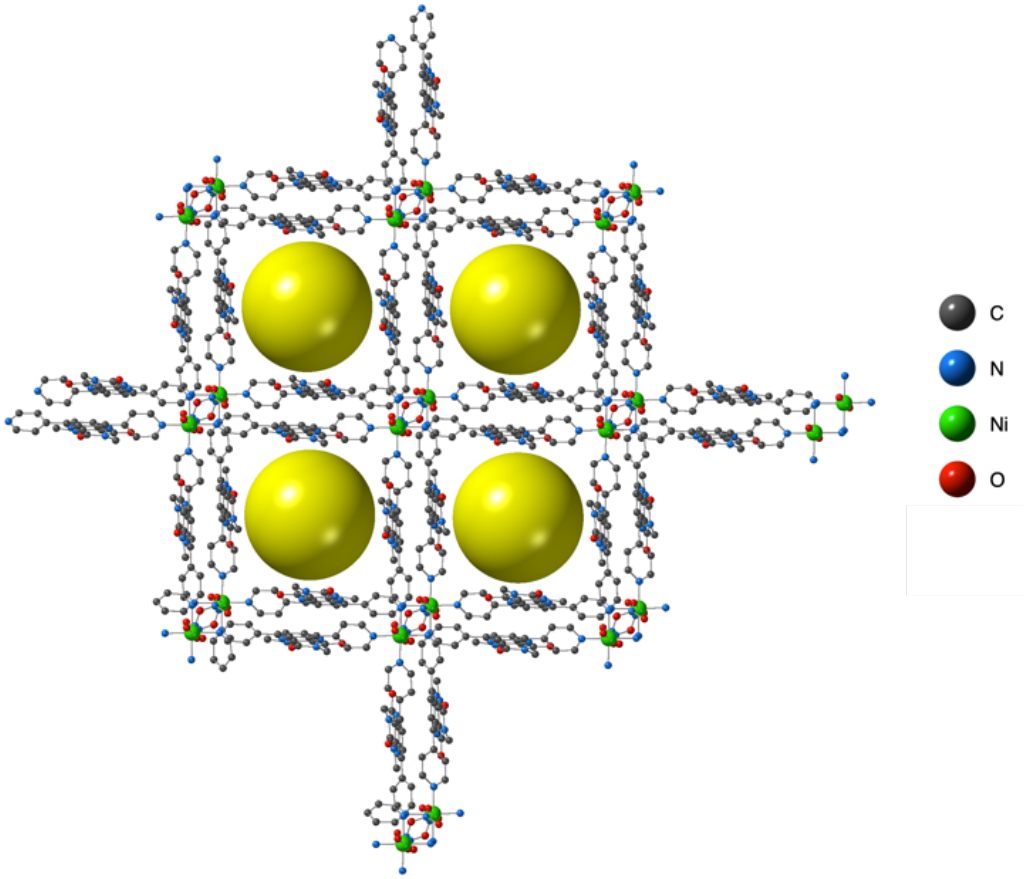

Figure 4: Representation of the structure of Ni**L1**$(NO_3)_2$, projection in the xOy planes. H atoms have been omitted for clarity. Yellow speres are representing the cavities. Disordered NO_3^- anions are not represented. Yellow spheres represent the cavities. For bond and distances see SI.

The EPR spectra of Cu**L1**$(NO_3)_2$ in the solid state has been recorded (see Figure S3 in SI). It is consistent with the presence of an octahedral Cu^{2+} paramagnetic species in the PCP.

When taken out of the solution, and as frequently observed for 2D coordination polymers, polycrystalline samples of Ni**L1**$(NO_3)_2$ and Cu**L1**$(NO_3)_2$ lose solvent molecules, which causes the sliding of the crystallographic planes, in accordance with the broadening

of the peaks of the XRPD diagrams (see Figure S4 in SI), in line with the amorphization of both polycrystalline compounds.

The electrochemical performances of the cathodes made from Cu**L1**$(NO_3)_2$ were preliminarily characterized by galvanostatic charge/discharge cycling (Figure S5 in SI). Interestingly, Li/MOF battery shows OCV of around 3.6 V. A first discharge shows that Li^+ can be inserted in Cu**L1**$(NO_3)_2$. A huge irreversible capacity loss is observed after the first discharge. However, even if nominal capacity is poor and progressive loss of capacity is observed with this MOF, our preliminary experiments proves that these compounds can be cycled in the presence of alkali cations.

In summary, three new Redox-active ligands **L1**-**L3** based on an alloxazine core have been designed, synthetized and characterized. Coordinating pyridyl fragment have been grafted on the phenyl ring of the alloxazine core, in different positions. For **L3**, the structure in the solid state has been elucidated. The electrochemical properties of the ligands have been studied in depth and evidenced the formation of a radical species by CV/EPR spectroscopy. The spin is mainly delocalized over the quinoxaline core as confirmed by DFT calculations. The coordination abilities of the ligand **L1** have been investigated, evidencing the formation of the first 3D coordination polymer based on alloxazine derivatives and 3d metals, that revealed high pi-stacking within the structure. Preliminarily galvanostatic charge/discharge cycling measurements were performed on the Cu-based CP, evidencing cationic (Li^+ and/or H^+) insertion during the reducing process. Future work should elucidate insertion/disinsertion mechanism and study structural evolution of the MOF during cycling.

Meanwhile, this preliminary study paves the way to synthesize MOF based on redox active ligands for application in the field of electrochemical energy storage.

ASSOCIATED CONTENT

Characterization techniques, Synthesis of **L1**-**L3**, synthesis of single crystals for **L3** and M**L1**$(NO_3)_2$, experimental methods and details, crystallographic Table for **L3** and Ni**L1**$(NO_3)_2$, figures and selected bonds for **L3** and Cu**L1**$(NO_3)_2$, XRPD and EPR and galvanostic charge discharge measurements for Cu**L1**$(NO_3)_2$. (DOC)

CCDC for **L3** : 2302867 and Ni**L1**$(NO_3)_2$: 2302868.

Author Contributions

Funding acquisition: S.F., M. D.-EM. and S. C.; experiments and data curation: J. C., D. P., A. J., N. L B., C. G. and S. L V.; investigation and interpretation of the results: all authors; writing of original draft: S. F. and S.C.; revision of the manuscript and additional contributions: all authors.

Funding Sources

ANR-20-CE05-0005

ANR-10-LABX-76-01

CNRS

Unistra

ITI Qmat

ACKNOWLEDGMENT

Financial support from the University of Strasbourg, the CNRS, Agence Nationale de la Recherche (ANR) through *BattAllox* Project ANR-20-CE05-0005 and STORE-EX Labex Project ANR-10-LABX-76-01 and ITI QMat are acknowledged. Nathalie Gruber (FR 2010) and Pr. Véronique Bulach (UMR 7140) are warmly acknowledged X-Ray diffraction resolution of the structures.

REFERENCES

(1) D'Alessandro, D. M. Exploiting redox activity in metal–organic frameworks: concepts, trends and perspectives. *Chem. Commun.* **2016**, *52* (58), 8957-8971, DOI: 10.1039/C6CC00805D.

(2) Ding, B.; Solomon, M. B.; Leong, C. F.; D'Alessandro, D. M. Redox-Active Ligands: Recent Advances towards Their Incorporation into Coordination Polymers and Metal-Organic Frameworks. *Coord. Chem. Rev.* **2021**, *439*, 213891, DOI: 10.1016/j.ccr.2021.213891.

(3) H. C. Zhou, J. R. Long, O. M. Yaghi, *Chem. Rev.* **2012**, *112*, 2, 673-674, Metal-organic frameworks special issue, DOI: 10.1021/cr300014x.

(4) Zhou, H.-C.; Kitagawa, S. Metal-organic frameworks (MOFs). *Chem. Soc. Rev.* **2014**, *43*, 5415-5418, DOI: 10.1039/C4CS90059F.

(5) M. Dincă, J. R. Long, *Chem. Rev*. **2020**, *120*, Porous framework chemistry special issue, DOI: 10.1021/acs.chemrev.0c00836

(6) Dhakshinamoorthy, A.; Asiri, A. M.; Garcia, H. Metal-Organic Framework (MOF) Compounds: Photocatalysts for Redox Reactions and Solar Fuel Production. *Angew. Chem., Int. Ed.* **2016**, *55*, 5414-5445, DOI: 10.1002/anie.201505581.

(7) Zheng, W.; Suk Lee, L. Y. Metal−Organic Frameworks for Electrocatalysis: Catalyst or Precatalyst? *ACS Energy Lett.* **2021**, 6, 8, 2838-2843, DOI: 10.1021/acsenergylett.1c01350.

(8) Stavila, V.; Talin, A. A.; Allendorf, M. D. MOF-based Electronic and Optoelectronic Devices. *Chem. Soc. Rev.***2014**, *43*, 5994-6010, DOI: 10.1039/C4CS00096J.

(9) Sun, L.; Campbell, M. G.; Dincă, M. Electrically Conductive Porous Metal-Organic Frameworks. *Angew. Chem., Int. Ed.* **2016**, *55*, 3566-3579, DOI: 10.1002/anie.201506219.

(10) Haldar, R.; Heinke, L.; Wöll, C. Advanced Photoresponsive Materials Using the Metal-Organic Framework Approach. *Adv. Mater.* **2020**, *32*, 1905227, DOI: 10.1002/adma.201905227.

(11) Tao, C.-a.; Li, Y.; Wang, J. The progress of electrochromic materials based on metal-organic frameworks. *Coord. Chem. Rev.* **2023**, *475*, 214891 DOI: 10.1016/j.ccr.2022.214891.

(12) Kan, W.-Q.; Wen, S.-Z.; He, Y.-C.; Xu, C.-Y. Viologen-Based Photochromic Coordination Polymers for Inkless and Erasable Prints. Inorg. Chem. 2017, 56, 14926-14935, DOI: 10.1021/acs.inorgchem.7b02206.

(13) Li, J. Y.; Zhang, S.; Gao, W.; Hua, Y.; Lian, H. Z. Guanidyl-functionalized magnetic bimetallic MOF nanocomposites developed for selective enrichment of phosphopeptides. *ACS Sustainable Chem. Eng.* **2020**, *8*, 16422-16429, DOI: 10.1021/acssuschemeng.0c04118.

(14) Weng, Y.-G.; Ren, Z.-H.; Zhang, Z.-R.; Shao, J.; Zhu, Q.-Y.; Dai, J. Tetrathiafulvalene-Cobalt Metal–Organic Frameworks for Lithium-Ion Batteries with Superb Rate Capability. *Inorg. Chem.* **2021**, *60*, 17074-17082, DOI: 10.1021/acs.inorgchem.1c02304.

(15) Solano, F.; Auban-Senzier, P.; Olejniczak, I.; Barszcz, B.; Runka, T.; Alemany, P.; Canadell, E.; Avarvari, N.; Zigon N. Bis(Vinylenedithio)-Tetrathiafulvalene-Based Coordination Networks *Chem. Eur. J.* **2023**, *29*, e202203138, DOI: 10.1002/chem.202203138

(16) Chua, C.; Doheny, P. W.; Ding, B.; Chan, B.; Yu, M.; Kepert, C. J.; D'Alessandro, D. M. Through-Space Intervalence Charge Transfer as a Mechanism for Charge Delocalization in Metal–Organic Frameworks. *J. Am. Chem. Soc.***2018**, *140*, 6622-6630, DOI: 10.1021/jacs.8b02638.

(17) Xie, L. S.; Skorupskii, G.; Dincă, M. Electrically Conductive Metal-Organic Frameworks. *Chem. Rev.* **2020**, *120*(16), 8536-8580, DOI: 10.1021/acs.chemrev.9b00766.

(18) Walsh, C. Naturally Occurring 5-Deazaflavin Coenzymes: Biological Redox Roles. *Acc. Chem. Res.* **1986**, *19*, 216-221, DOI: 110.1021/ar00127a004.

(19) Flavins: Photochemistry and Photobiology, ed. E. Silva and A. M. Edwards, RSC Publishing, 2006.

(20) Kaim, W.; Schwederski, B.; Heilmann, O.; Hornung, F. M. Coordination Compounds of Pteridine, Alloxazine and Flavin Ligands: Structures and Properties. *Coord. Chem. Rev.* **1999**, *182*, 323-342, DOI: 10.1016/S0010-8545(98)00193-3.

(21) Mouli, M. S. S. V.; Mishra A. K. Divergent Crystallographic Architecture for Silver-Flavin Complexes Induced via pH Variation *Chemistryselect*, **2022**, *7*, e202202126, 10.1002/slct.20220212.

(22) Mouli, M. S. S. V.; Mishra A. K. Formation of the silver-flavin coordination polymers and their morphological studies *CrystEngComm*, **2022**, *24*, 2221-2225, DOI : 10.1039/D2CE00071G.

(23) Hong, J.; Lee, M.; Lee, B.; Seo, D.-H.; Park, C. B.; Kang, K. Biologically inspired pteridine redox centres for rechargeable batteries. *Nat. Commun.* **2014**, *5*, 5335, DOI: 10.1038/ncomms6335.

(24) Lin, K.; Gomez-Bombarelli, R.; Beh, E. S.; Tong, L.; Chen, Q.; Valle, A.; Aspuru-Guzik, A.; Aziz, M. J.; Gordon, R. G.A Redox-Flow Battery with an Alloxazine-Based Organic Electrolyte. *Nat. Energy* **2016**, *1*, 16102, DOI: 10.1038/nenergy.2016.102.

(25) Das, A;. Jobelius, H;. Schleinitz, J;. Gamboa-Ramirez, S;. Creste, G.; Kervern, G;. Raya, J.; Le Breton, N.; Guénet, A;. Boubegtiten-Fezoua, Z.; Grimaud, L;. Orio, M.; Rogez, G.; Hellwig, P;. Choua, S.; Ferlay, S.; Desage-El Murr, M. A hybrid bioinspired catechol-alloxazine triangular

nickel complex stabilizing protons and electrons *Inorg. Chem. Front*., **2021**, *8*, 5286-5298 DOI: 10.1039/D1QI01131F.

(26) Das, A.; Schleinitz, J.; Karmazin, L.; Vincent, B.; Le Breton, N.; Rogez, G.; Guénet, A.; Choua, S.; Grimaud, L.; Desage-El Murr, M. A Single Bioinspired Hexameric Nickel Catechol-Alloxazine Catalyst Combines Metal and Radical Mechanisms for Alkene Hydrosilylation *Chem. Eur. J.* **2022**, *28*, e202200596, DOI: 10.1002/chem.202200596.

(27) Ertan, A.; Koziol, J. Structure of 1,3,9-trimethyl- alloxazine, *Acta Crystallogr., Sect. C: Cryst. Struct. Commun*., **1993**, *49*, 2179-2181, DOI: 10.1107/S0108270193005803.

(28) Clarke, M. J.; Dowling, M. G. Cyclic voltammetry studies of metalloflavin complexes in aqueous solution Inorg. Chem. **1981**, 20, 3506-3514, DOI: 10.1021/ic50224a070.

(29) Hornung, F. M;. Heilmann, O.; Kaim, W.; Zalis, S.; Fiedler, J. Metal vs Ligand Reduction in Complexes of 1,3-Dimethylalloxazine (DMA) with Copper(I), Ruthenium(II), and Tungsten(VI). Crystal Structures of (DMA)WO_2Cl_2 and (Bis(1-methylimidazol-2-yl)ketone)WO_2Cl_2 *Inorg. Chem*. **2000**, *39*, 4052-4058, DOI: 10.1021/ic0001816.

(30) Spek, A. L. Single-crystal structure validation with the program PLATON *J. Appl. Crystallogr*. 2003, 36, 7-13, DOI: 10.1107/S0021889802022112

SYNOPSIS.

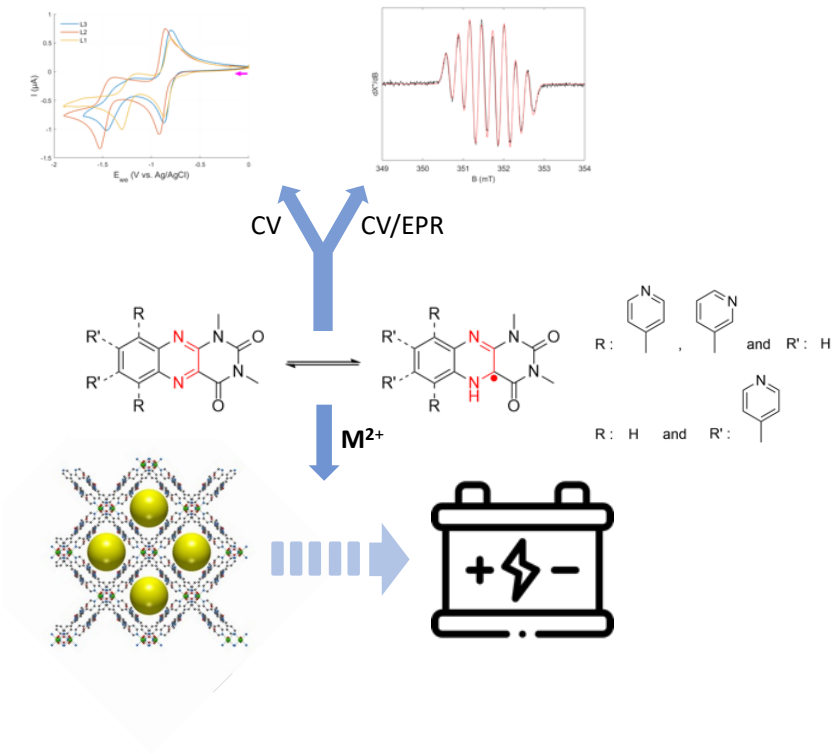

Formation of the first Redox-active Coordination Polymers based on the alloxazine core.